

## Optical-Absorption Intensities of Rare-Earth Ions in Crystals: the Absorption Spectrum of Thulium Ethyl Sulfate\*

WILLIAM F. KRUPKE†

*Aerospace Corporation, El Segundo, California*

AND

JOHN B. GRUBER

*Department of Physics, University of California, Los Angeles, California*

(Received 14 April 1965; revised manuscript received 17 May 1965)

Absolute intensities of the electronic transitions occurring in the absorption spectrum of thulium ethyl sulfate have been measured at 4.2 and 23°K. In addition, absolute intensities due to vibronic and electronic transitions have been measured at 300°K. The oscillator strengths of electric-dipole transitions between individual crystalline Stark-split components which were observed at 23°K are compared with theoretical calculations and the results are discussed. The total electric-dipole oscillator strengths measured at 300°K are compared with theoretical calculations and also with the low-temperature results. The observed intensities, which vary as much as 40-fold between 38 000 cm<sup>-1</sup> and 15 000 cm<sup>-1</sup>, can be accounted for by using only several phenomenological parameters. Interpretation of the parameters is discussed in terms of excited-electronic-state wave functions and their admixture into the ground-state electronic configuration.

### INTRODUCTION

ALTHOUGH considerable progress has been made in interpreting the optical spectra of rare-earth ions embedded in crystalline solids,<sup>1-6</sup> only recently has sufficient knowledge been acquired regarding the interaction of the localized *f* electrons with the lattice environment to make possible a detailed study of the intensities of the observed spectra. Recently, Judd<sup>7</sup> and Ofelt<sup>8</sup> independently have discussed a general theoretical framework for understanding the intensities of the optical transitions. The satisfying agreement found between calculated and measured oscillator strengths for solutions of rare-earth ions prompted Axe<sup>9</sup> to examine the theory in more detail by considering the relative intensities of the observed electric- and magnetic-dipole fluorescence spectrum of europium ethyl sulfate single crystals. By reasoning that certain observed transitions were pure magnetic-dipole transitions whose intensities were independent of the crystalline

Stark field, Axe was able to relate measured relative fluorescence intensities to absolute intensities. However, to accurately calculate absolute intensities, states of all multiplicities must be included. Such a calculation for Eu<sup>3+</sup> would be quite difficult owing to the large number of states<sup>10</sup> whose inclusion will contribute to the intensities.

Absolute intensities can be measured directly with greater accuracy and ease in absorption spectra. While the absorption intensities of infrared transitions of several rare-earth chlorides have been reported recently,<sup>11</sup> no detailed examination of transitions between individual Stark components has been carried out. In this paper we report the results of such a study for the transitions observed in the absorption spectrum of thulium ethyl sulfate.

The trivalent thulium ion was chosen because it has a relatively simple ground-state electronic configuration of 4*f*<sup>12</sup> with a number of *J* levels found throughout the ultraviolet and visible region that are well separated and well identified.<sup>12,13</sup> The simplicity of this configuration allows one to handle the calculations with rigor, yet it is complex enough to fully test the theoretical framework. The ethyl sulfate lattice was chosen, in spite of the difficulties to be discussed later, because the Tm<sup>3+</sup> site symmetry is well known and because the crystalline Stark splitting of the *J* levels is well understood and has been the subject of a number of investigations.<sup>14-16</sup> By using undiluted crystals we avoided

\* This research was supported by the U. S. Air Force under Contract No. AF04(695)-469 and in part by the U. S. Atomic Energy Commission under Contract No. AT(1101)-34, Project No. 120.

† Predoctoral research assistant, Department of Physics, University of California at Los Angeles.

<sup>1</sup> G. H. Dieke and H. M. Crosswhite, *Appl. Optics* **2**, 675 (1963).

<sup>2</sup> B. R. Judd, *Operator Techniques in Atomic Spectroscopy* (McGraw-Hill Book Company, Inc., New York, 1963).

<sup>3</sup> B. G. Wybourne, *Spectroscopic Properties of Rare Earths* (Interscience Publishers, Inc., New York, 1965).

<sup>4</sup> W. A. Runciman and B. G. Wybourne, *J. Chem. Phys.* **31**, 1149 (1959); J. B. Gruber and J. G. Conway, *ibid.* **32**, 1178 (1960); **32**, 1531 (1960); J. S. Margolis, *ibid.* **35**, 1367 (1961); E. M. Carlson and G. H. Dieke, *ibid.* **34**, 1602 (1961).

<sup>5</sup> K. H. Hellwege, S. Hüfner, and H. G. Kahle, *Z. Physik* **160**, 149 (1960); S. Hüfner, *ibid.* **169**, 417 (1962); F. H. Spedding, W. J. Haas, W. L. Sutherland, and C. A. Eckroth, *J. Chem. Phys.* **42**, 981 (1965).

<sup>6</sup> I. Richman, R. A. Satten, and E. Y. Wong, *J. Chem. Phys.* **39**, 1833 (1963).

<sup>7</sup> B. R. Judd, *Phys. Rev.* **127**, 750 (1962).

<sup>8</sup> G. S. Ofelt, *J. Chem. Phys.* **37**, 511 (1962).

<sup>9</sup> J. D. Axe, Jr., *J. Chem. Phys.* **39**, 1154 (1963).

<sup>10</sup> N. C. Chang and J. B. Gruber, *J. Chem. Phys.* **41**, 3227 (1964).

<sup>11</sup> F. Varsanyi and G. H. Dieke, *J. Chem. Phys.* **36**, 835 (1962).

<sup>12</sup> J. B. Gruber and J. G. Conway, *J. Chem. Phys.* **32**, 1178 (1960).

<sup>13</sup> J. B. Gruber, W. F. Krupke, and J. M. Poindexter, *J. Chem. Phys.* **41**, 3363 (1964).

<sup>14</sup> U. Johnsen, *Z. Physik* **152**, 454 (1958).

<sup>15</sup> J. B. Gruber and J. G. Conway, *J. Chem. Phys.* **32**, 1531 (1960).

<sup>16</sup> E. Y. Wong and I. Richman, *J. Chem. Phys.* **34**, 1182 (1961).

uncertainty in the concentration of  $\text{Tm}^{3+}$  since the number of ions per  $\text{cm}^3$  is needed to determine the absolute values of the intensities. Although the theoretical framework has been discussed previously,<sup>7,8</sup> it is worthwhile to review certain aspects of the theory and to express the results in a form more suitable for our calculations.

### THEORETICAL CONSIDERATIONS

If a photon from a collimated beam of incident black-body radiation is absorbed by a tightly bound  $4f$  electron of a rare-earth ion in a crystalline lattice, the integrated absorption coefficient, representing an electronic transition within the  $4f^n$  configuration, may be written as

$$\int_0^\infty k(\nu) d\nu = \rho \frac{(n^2+2)^2}{9n} \frac{8\pi^3\nu}{3ch} \left| \sum_{i,j} \langle i | \mathbf{P} | j \rangle \right|^2, \quad (1)$$

where  $\rho$  represents the number of rare earth ions per cubic centimeter,  $c$  is the speed of light,  $h$  is Planck's constant, and  $n$  is the index of refraction of the bulk isotropic dielectric medium at the frequency  $\nu$  of the photon involved in the transition.<sup>17-19</sup> In Eq. (1),  $\mathbf{P}$  is the electric-dipole-moment operator  $\mathbf{P} = -e \sum_i \mathbf{r}_i$  for a transition between the ground electronic state  $i$  and some excited state  $j$ . The matrix elements of the electric-dipole operator between two states  $i$  and  $j$  will be nonzero only if  $i$  and  $j$  do not have the same parity. Since the wave functions used to describe the levels of the  $4f^n$  configuration, usually written as a linear combination of states  $|\gamma f^n(SL)\rangle$ ,<sup>20</sup>

$$|\gamma f^n(SL)J\rangle = \sum_{S,L} A(S,L,J) |\gamma f^n(SL)\rangle, \quad (2)$$

have the same parity, states of opposite parity must be mixed into the wave functions associated with at least one of the two levels considered. This may be achieved if the environment of the ion in the crystal is such that its nucleus is not situated at a center of inversion. The crystalline Stark field produced by the lattice charges at the site of the  $4f$  electrons not only has the effect of removing (at least partially) the degeneracy of a given  $J$  level, but also has the effect of mixing a small amount of opposite-parity excited

orbital wave functions into the  $4f^n$  states. For electric-dipole transitions between individual crystalline Stark-split components, the odd-parity part of the crystalline Stark potential is considered as the mechanism for mixing the parity of the states. Under this assumption, the electronic states of the ion in the lattice may be written as

$$|\gamma 4f^n[SL]J,\mu\rangle = |\Psi_0\rangle + \sum_{\gamma' 4f^{n-1}n'l'} \langle \gamma' 4f^{n-1}n'l' | V_{\text{odd}} | \Psi_0 \rangle |\gamma' 4f^{n-1}n'l'\rangle / \Delta E, \quad (3)$$

where  $|\Psi_0\rangle = \sum_{J_z} A(\mu, J_z) |\gamma 4f^n[SL]JJ_z\rangle$ ,  $\Delta E$  is the energy difference between excited states and  $4f^n$  states, and  $\bar{\mu}^{21}$  the crystal quantum number.<sup>5,22</sup> The  $A(\mu, J_z)$  coefficients corresponding to a given  $[SL]$ ,  $J$  state are determined from a first-order degenerate perturbation calculation, using the  $|\gamma f^n[SL]J\rangle$  wave functions as zero-order wave functions. The coefficients  $A(\mu, J_z)$  are specified by the even-term part of the crystalline-Stark-field perturbation Hamiltonian. The second term in (3) is summed over all excited configurations  $4f^{n-1}n'l'$  for  $l'$  even, where  $n'$  and  $l'$  are the principal and orbital quantum numbers of the excited rare-earth electronic configuration.

The extent to which one may invoke closure in evaluating the expectation value of the electric dipole operator  $P_q^{(1)}$  between such perturbed  $4f^n$  states depends on the extent to which the energy denominators are independent of summation indices. Maximum simplification results if all contributing excited configurations are completely degenerate.<sup>23</sup> Under this assumption, the value of the electric-dipole matrix is just the value of the operator  $P_q^{(1)} C_p^{(k)}$  between unperturbed  $4f^n$  states [See Ofelt's Eq. 27].<sup>8</sup> While this assumption completely obviates the need to evaluate intraradial integrals, it does not correspond to the actual physical situation, even for the free ion.<sup>24</sup>

A less restrictive and physically more realistic assumption is that each excited orbital is completely degenerate in  $S$ ,  $L$ , and  $J$ , but each is separated in energy from the  $4f^n$  configuration by an amount characteristic of that particular orbital. Expanding Judd's Eq. (13),<sup>7</sup> which is based on this assumption, to a form more suitable for comparing calculated with observed intensities, one obtains the equation,

$$\begin{aligned} \langle \gamma f^n[SL]J,\mu | P_q^{(1)} | \gamma f^n[S'L']J'\mu' \rangle &= \sum_{\text{todd } p>0} \sum_{J_z} \sum_{J_z'} \sum_{J_z''} A(\mu, J_z) A(\mu', J_z') (-1)^{J-J_z} \sum_{\lambda=2,4,6} (2\lambda+1) A_{t,p} \Xi(t,\lambda) \Gamma^{(\lambda)} \\ &\times \left[ \begin{pmatrix} J' & J & \lambda \\ J_z' & -J_z & (p+q) \end{pmatrix} \begin{pmatrix} t & 1 & \lambda \\ p & q & -(p+q) \end{pmatrix} + (-1)^p \begin{pmatrix} J' & J & \lambda \\ J_z' & -J_z & (q-p) \end{pmatrix} \begin{pmatrix} t & 1 & \lambda \\ -p & q & (p-q) \end{pmatrix} \right], \quad (4) \end{aligned}$$

<sup>17</sup> W. B. Fowler and D. L. Dexter, *Phys. Rev.* **128**, 2154 (1962).

<sup>18</sup> A. C. G. Mitchell, M. W. Zemansky, *Resonance Radiation and Excited Atoms* (University Press, Cambridge, England, 1961).

<sup>19</sup> L. J. F. Broer, C. J. Gorter, and J. Hoogschagen, *Physica* **11**, 231 (1945).

<sup>20</sup> Quantum numbers useful in classifying states, but which in themselves are not exact quantum numbers, are enclosed in square brackets. Additional quantum numbers not specified are represented by  $\gamma$ .

<sup>21</sup> In  $D_{3h}$  symmetry for example, crystalline Stark states are combinations of  $J_z = M_J \pm 6n$  ( $n=0, 1, 2, \dots$ ) and are labeled  $\bar{\mu} = 0, \pm 1, \pm 2$ , and 3.

<sup>22</sup> K. H. Hellwege, *Ann. Physik* **4**, 95 (1949).

<sup>23</sup> J. S. Griffith, *Mol. Phys.* **3**, 477 (1960).

<sup>24</sup> G. H. Dieke, H. M. Crosswhite, and B. Dunn, *J. Opt. Soc. Am.* **51**, 820 (1961).

where the expressions for  $A_{t,p}$  and  $\Xi(t,\lambda)$  have been given earlier<sup>7</sup> and where

$$\Gamma^{(\lambda)} = \sum_{S,L} \sum_{S',L'} A(SLJ)A(S'L'J') \langle \gamma f^n SLJ || U^{(\lambda)} || \gamma f^n S'L'J' \rangle. \quad (5)$$

To carry out the summations, the symmetry of the crystalline Stark field must be specified. In ethyl sulfate lattices, it is well known that the rare-earth ion occupies a site of  $C_{3h}$  symmetry and that the nearest-neighbor oxygen atoms of the water molecules of hydration form a slightly more symmetric configuration  $D_{3h}$  symmetry about the rare-earth ion.<sup>25,26</sup> The assumption of a  $D_{3h}$  symmetry potential has been successful in interpreting optical and resonance spectra of rare-earth ethyl sulfates.<sup>4,5,27,28</sup> The odd-parity terms in the expansion of  $V_{D_{3h}}$  are

$$V_{D_{3h}} = A_{3,3} 3^3 V_{3,3} + A_{5,3} 3^5 V_{5,3} + A_{7,3} 3^7 V_{7,3}. \quad (6)$$

In this symmetry, there will be at most five adjustable parameters describing transition strengths, namely,  $A_{33\Xi}(3,2)$ ,  $A_{33\Xi}(3,4)$ ,  $A_{53\Xi}(5,4)$ ,  $A_{53\Xi}(5,6)$ , and  $A_{73\Xi}(7,6)$ . One may evaluate the matrix elements of Eq. (4) and obtain

$$\begin{aligned} & \langle \gamma 4 f^n [SL] J, \mu | P_{+1}^{[1]} | \gamma 4 f^n [S'L'] J', \mu' \rangle \\ &= \sum_{J_z, J_z'} A(\mu, J_z) A'(\mu', J_z') (-1)^{J-J_z'} \left\{ -5 \left( \frac{1}{7} \right)^{1/2} \begin{pmatrix} J' & J & 2 \\ J_z' & -J_z & -2 \end{pmatrix} A_{33\Xi}(3,2) \Gamma^{(2)} \right. \\ & \quad + 3 \left[ \begin{pmatrix} J' & J & 4 \\ J_z' & -J_z & 4 \end{pmatrix} - \frac{1}{2} \left( \frac{1}{7} \right)^{1/2} \begin{pmatrix} J' & J & 4 \\ J_z' & -J_z & -2 \end{pmatrix} \right] A_{33\Xi}(3,4) \Gamma^{(4)} \\ & \quad + \left( \frac{9}{55} \right)^{1/2} \left[ \begin{pmatrix} J' & J & 4 \\ J_z' & -J_z & 4 \end{pmatrix} - 2(7^{1/2}) \begin{pmatrix} J' & J & 4 \\ J_z' & -J_z & -2 \end{pmatrix} \right] A_{53\Xi}(5,4) \Gamma^{(4)} \\ & \quad + \left( \frac{13}{11} \right)^{1/2} \left[ \left( \frac{15}{2} \right)^{1/2} \begin{pmatrix} J' & J & 6 \\ J_z' & -J_z & 4 \end{pmatrix} - \begin{pmatrix} J' & J & 6 \\ J_z' & -J_z & -2 \end{pmatrix} \right] A_{53\Xi}(5,6) \Gamma^{(6)} \\ & \quad \left. + \frac{13}{7} \left( \frac{21}{13} \right)^{1/2} \left[ \begin{pmatrix} J' & J & 6 \\ J_z' & -J_z & 4 \end{pmatrix} \left( \frac{2}{15} \right)^{1/2} - \begin{pmatrix} J' & J & 6 \\ J_z' & -J_z & -2 \end{pmatrix} \right] A_{73\Xi}(7,6) \Gamma^{(6)} \right\}, \quad (7) \end{aligned}$$

and

$$\begin{aligned} & \langle \gamma 4 f^n [SL] J, \mu | P_0^{[1]} | \gamma 4 f^n [S'L'] J', \mu' \rangle \\ &= \sum_{J_z, J_z'} A(\mu, J_z) A'(\mu', J_z') (-1)^{J-J_z'} \left\{ \frac{3}{2} \left[ \begin{pmatrix} J' & J & 4 \\ J_z' & -J_z & 3 \end{pmatrix} - \begin{pmatrix} J' & J & 4 \\ J_z' & -J_z & -3 \end{pmatrix} \right] \right. \\ & \quad \times \left[ A_{33\Xi}(3,4) - 8 \left( \frac{1}{55} \right)^{1/2} A_{53\Xi}(5,4) \right] \Gamma^{(4)} + \frac{3}{2} \left( \frac{26}{11} \right)^{1/2} \left[ \begin{pmatrix} J' & J & 6 \\ J_z' & -J_z & 3 \end{pmatrix} - \begin{pmatrix} J' & J & 6 \\ J_z' & -J_z & -3 \end{pmatrix} \right] \\ & \quad \left. \times \left[ -A_{53\Xi}(5,6) + \frac{4}{3} \left( \frac{11}{21} \right)^{1/2} A_{73\Xi}(7,6) \right] \Gamma^{(6)} \right\}. \quad (8) \end{aligned}$$

An equation similar to Eq. (7) is found for  $\langle |P_{-1}^{[1]}| \rangle$ , whose absolute value is equal to  $\langle |P_{+1}^{[1]}| \rangle$  for any  $\bar{\mu}, \bar{\mu}'$ . In  $D_{3h}$  symmetry the crystal quantum number<sup>5,19</sup> is designated by  $\bar{\mu}, \bar{\mu}'$ .

Equations (7) and (8) are in a general form suitable for the evaluation of the matrix elements for electric-dipole transitions between any two Stark components

of a rare-earth ion in a site having  $D_{3h}$  symmetry. When the initial and final crystalline Stark levels are diagonal in  $J_z$  (i.e.  $A(\mu, J_z) = 1$ ,  $A(\mu', J_z') = 1$ ), the resulting expression is identical to Axe's Eq. (7) [Ref. 9] which he obtained from Judd's treatment of the problem.<sup>7</sup>

#### EXPERIMENTAL DETAILS

Single crystals of the pure salt were prepared as previously reported.<sup>12</sup> The absorption spectrum was taken with a 21-foot Wadsworth mount grating spectrograph having a dispersion of 2.6 Å/mm in the first

<sup>25</sup> J. A. A. Ketelaar, *Physica* **4**, 619 (1937).

<sup>26</sup> D. R. Fitzwater and R. E. Rundle, *Z. Krist.* **112**, 362 (1959).

<sup>27</sup> E. V. Sayre and S. Freed, *J. Chem. Phys.* **24**, 1213 (1956).

<sup>28</sup> R. J. Elliott and K. W. H. Stevens, *Proc. Roy. Soc. (London)* **A219**, 387 (1953).

order, and with a Bausch and Lomb spectrograph having a dispersion of  $8.1 \text{ \AA/mm}$  in the first order. The ultraviolet spectrum was studied in the second order with both instruments. A Sylvania hydrogen arc lamp was used as the ultraviolet source and iron arc lines served as standards. All intensity measurements were made on a Cary 14 spectrophotometer, which provides a nearly collimated signal radiation flux, and an automatically constant signal source intensity obtained by means of a reference beam and variable slit control.

For the intensity measurements, two clear crystals about  $7 \times 10 \text{ mm}$  in area were polished so as to have flat, parallel faces. The crystals were  $0.250 \pm 0.003 \text{ cm}$  and  $0.191 \pm 0.003 \text{ cm}$  in thickness. From the measured weight and volume, the density of the single crystals was found to be  $1.90 \pm 0.05 \text{ g/cc}$  which gives a  $\text{Tm}^{3+}$  ion density of  $1.61 \times 10^{21} \text{ ions/cc}$ . The spectrum was studied at  $4.2^\circ\text{K}$  and  $23^\circ\text{K}$  using the thicker crystal, but the spectrum at room temperature was studied using the thinner crystal. For the  $4.2^\circ\text{K}$  measurements, the crystal was mounted on a baffle (mask) and immersed directly in liquid helium. For measurements at higher temperatures, (i.e.,  $23$  and  $300^\circ\text{K}$ ), the sample was suitably masked and mounted on the coldfinger of a liquid-helium conduction Dewar. During the experiments, the equilibrium temperature maintained by the crystal was  $23 \pm 1^\circ\text{K}$  as measured by a thermocouple attached to the side of the crystal. As a check, the integrated absorption coefficients of transitions originating from the ground crystalline Stark level were measured at  $4.2^\circ\text{K}$  (immersion) and at the  $23 \pm 1^\circ\text{K}$  temperature. If a Boltzman population distribution is assumed, the measured change in the integrated absorption coefficients agrees quite well with the assertion that the higher temperature spectrum was measured at  $T = 23^\circ\text{K}$ . The  $1^\circ\text{K}$  error in the equilibrium temperature could result in as much as  $7\%$  discrepancy in intensities between transitions originating from the ground and first excited crystalline Stark levels.

Using careful techniques, no trace of clouding due to dehydration was observed when the crystal was placed in the evacuated chamber of the conduction Dewar and cooled to low temperatures. For absorption at wavelengths less than  $6600 \text{ \AA}$ , the Cary-14 provides a monochromatic signal beam (predispersed); consequently, very little heating of the sample was observed during the experiments. For the  ${}^3F_4$  and  ${}^3F_3$  absorption spectrum, however, the Cary infrared source and detector were required. Since the signal beam is not predispersed in this wavelength region, heating of the crystal precluded the recording of quantitatively useful data for these groups. Polarization spectra were obtained throughout the visible and ultraviolet spectral region with a large-aperture Glan (air space) polarizer.

At  $300^\circ\text{K}$ , transitions were observed from nearly all the  ${}^3H_6$  Stark levels to all levels except  ${}^1S_0$ ,  ${}^3H_4$ , and  ${}^3H_5$  levels. Heating of the sample with the undispersed infrared signal beam is small compared to  $kT$ .

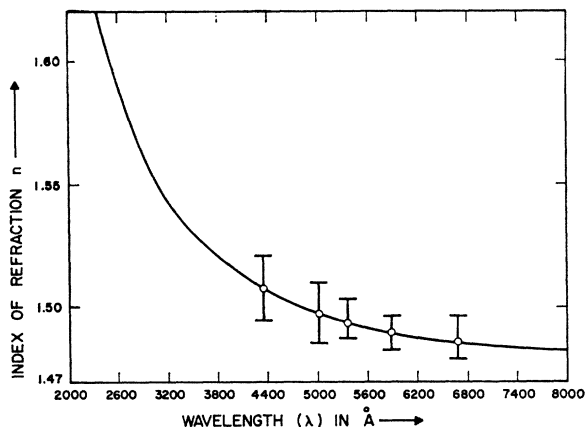


FIG. 1. The index of refraction ( $n$ ) of thulium ethyl sulfate versus wavelength ( $\lambda$ ). The uncertainty in the measured value for the index of refraction is approximately several percent at the five different wavelengths mentioned in the text. Within this uncertainty no difference in indices for the ordinary and extraordinary rays could be determined.

For the low-temperature intensity measurements the slit resolution was equal to the slit mismatch of the instrument, which varied from  $0.6 \text{ cm}^{-1}$  to  $3 \text{ cm}^{-1}$ . The linewidths of the TmES spectrum at low temperatures varied from  $5 \text{ cm}^{-1}$  to  $30 \text{ cm}^{-1}$  and for all the lines utilized in this study, the slit width was generally more than twice as narrow as the linewidths of the measured lines. Errors in determining the transition strength arise not only from instrumental errors in measuring a prescribed area, but also in determining the base-line for a given transition, due to the presence of nearby transitions. The former error is believed not to exceed  $1\%$  for the magnitude of the areas measured, while the base-line errors due to the presence of nearby transitions in the worst case may be as large as  $25\%$ . For the measurements reported in this paper, the average error due to uncertainty in the base-line is approximately  $10\%$ .

Single crystals of thulium ethyl sulfate are not isotropic, but the difference in indices for the ordinary and extraordinary rays amounts to less than the several percent uncertainty in the values of  $n$  measured. Experimental values for  $n$  were measured at  $4358.3$ ,  $5015.7$ ,  $5460.8$ ,  $5875.6$ , and  $6678.2 \text{ \AA}$  by the method of minimum deviation. To within several percent, the wavelength dependence of the index of refraction follows a simple Cauchy dispersion equation for  $n(\lambda) = a + b/\lambda^2$  throughout the visible region and is assumed to hold reasonably well in the near ultraviolet. The experimental index of refraction as a function of wavelength is compared with the Cauchy dispersion curve in Fig. 1.

#### OBSERVED ABSORPTION SPECTRUM

The absorption spectrum of pure thulium ethyl sulfate crystals several mm thick contains more lines than

TABLE I. Ultraviolet absorption spectrum of  $\text{Tm}(\text{C}_2\text{H}_5\text{SO}_4)_3 \cdot 9\text{H}_2\text{O}$  at 77°K.

Empirical designation	Wavelength in Å (in air)	Wavenumber in $\text{cm}^{-1}$ , (in vacuum)	Polarization	Transitions from Stark components of the groundstate level, ${}^3H_6^a$	Excited $SLJ$ -level assignment
$G_1$	3617.7	27 634.0	$\sigma$	$\pm 2 \rightarrow \pm 2$	${}^1D_2$
$G_2$	3612.4	27 674	$\sigma$	$3 \rightarrow \pm 1$	
$G_3$	3608.2	27 706.8	$\pi$	$\pm 1 \rightarrow \pm 2$	
$G_4$	3598.9	27 778.4	$\sigma$	$\pm 1 \rightarrow \pm 1$	
$G_5$	3596.7	27 795.4	$\sigma$	$\pm 2 \rightarrow \pm 2$	
$G_6$	3587.6	27 865.9	$\pi$	$\pm 2 \rightarrow \pm 1$	
$G_7$	3586.5	27 873.9	$\pi$	$\pm 1 \rightarrow \pm 2$	
$G_8$	3582.4 <sup>b</sup>	27 906.3	$\sigma$	$0 \rightarrow \pm 2$	
$G_9$	3577.4	27 945.3	$\sigma$	$\pm 1 \rightarrow \pm 1$	
$H_1$	2885.7	34 643.9	$\pi$	$\pm 1 \rightarrow \pm 2$	
$H_2$	2883.5	34 670.0	$\sigma$	$\pm 1 \rightarrow 3$	
$H_3$	2881.0	34 700.1	$\pi$	$\pm 1 \rightarrow \pm 2$	${}^1I_6$
$H_4$	2869.1 <sup>b</sup>	34 843.9	$\sigma$	$0 \rightarrow \pm 2$	
$H_5$	2866.9 <sup>b</sup>	34 870.6	$\pi$	$0 \rightarrow 3$	
$H_6$	2864.5 <sup>b</sup>	34 899.9	$\sigma$	$0 \rightarrow \pm 2$	
$I_1$	2845.2	35 137.0	$\pi$	$3 \rightarrow 0$	
$I_2$	2842.8	35 164.6	$\sigma$	$\pm 2 \rightarrow 0$	${}^3P_0$
$I_3$	2829.8	35 327.8	$\sigma$	$\pm 2 \rightarrow 0$	
$J_1$	2767.4	36 124.4	$\sigma$	$\pm 2 \rightarrow 0$	${}^3P_1$
$J_2$	2761.0	36 208.8	$\pi$	$\pm 2 \rightarrow \pm 1$	
$J_3$	2755.1	36 285.6	$\sigma$	$\pm 1 \rightarrow \pm 1$	
$J_4$	2754.8	36 289.5	$\sigma$	$\pm 2 \rightarrow 0$	
$J_5$	2748.4	36 374.1	$\pi$	$\pm 2 \rightarrow \pm 1$	
$J_6$	2742.5	36 452.3	$\sigma$	$\pm 1 \rightarrow \pm 1$	
$K_1$	2639.8	37 870.4	$\sigma$	$\pm 2 \rightarrow \pm 2$	${}^3P_2$
$K_2$	2636.9	37 911.5	$\pi$	$\pm 2 \rightarrow \pm 1$	
$K_3$	2634.5	37 946.6	$\pi$	$\pm 1 \rightarrow \pm 2$	
$K_4$	2631.6	37 987.1	$\sigma$	$\pm 1 \rightarrow \pm 1$	
$K_5$	2630.2	38 008.6	$\sigma$	$3 \rightarrow \pm 1$	
$K_6$	2628.5	38 033.2	$\sigma$	$\pm 2 \rightarrow \pm 2$	
$K_7$	2623.0	38 112.9	$\pi$	$\pm 1 \rightarrow \pm 2$	
$K_8$	2620.8 <sup>b</sup>	38 144.9	$\sigma$	$0 \rightarrow \pm 2$	
$K_9$	2620.2	38 153.6	$\sigma$	$\pm 1 \rightarrow \pm 1$	
$K_{10}$	2617.0	38 200.3	$\sigma$	$\pm 2 \rightarrow 0$	

<sup>a</sup> The crystal quantum states of the  $f^{12}$  wavefunctions are mixtures of  $J_2 = MJ \pm 6n$  ( $n = 0, 1, 2, 3 \dots$ ). The corresponding crystal quantum labels for these states are  $\bar{m} = 0, \pm 1, \pm 2$ , and 3.

<sup>b</sup> Level persists at 4.2°K.

can be accounted for solely on the basis of electronic electric-dipole transitions. Many of these additional lines are due to combinations of transitions to excited ionic states and changes of the vibrational state of the surrounding ion complex or the crystal lattice. To distinguish between these two different types of transitions, the spectrum was studied in detail at 4.2, 77, and at 300°K. The  ${}^3P_J$  levels and the  ${}^1D_2$  levels are well separated so that the temperature-dependent spectrum which yields information on the crystalline Stark splitting of the ground-state  ${}^3H_6$  level may be studied in detail. Since selection rules forbid many electronic transitions at 4.2°K, it is the 77°K spectrum that allows one to establish most of the Stark components of excited states. Unless vibronic and crystalline Stark levels coincide within the limit of resolution, it is usually possible to distinguish which are vibronic in origin by the repetition of such vibrational levels coupled to the various electronic states.

It is not possible to observe the complete vibration energy spectrum by studying the  ${}^3P_0$  level alone since vibronic-electronic transitions have selection rules.<sup>6</sup>

For this reason, it is necessary to study the vibrational spectra associated with other levels such as the  ${}^3P_1$  and  ${}^3P_2$  levels. Since the crystalline field splits these levels into Stark components, the vibrational spectra overlap; however, the vibrational energy levels can be obtained by the method of constant differences.

The lowest-lying vibrational levels above the ground state ( ${}^3H_6, \bar{m} = 0$ ) are found at 20, 35, 52, and 58  $\text{cm}^{-1}$ . At 23°K the vibronic transitions still observed using the thinnest possible crystals for the intensity measurements were usually resolved from the electronic transitions taking place from the first excited Stark level  $\bar{m} = \pm 1$  at 32  $\text{cm}^{-1}$ .

In general, the observed vibrational spectrum associated with the  ${}^3P_J$  and  ${}^1D_2$  levels is an order of magnitude weaker than the allowed electric-dipole transitions. However, in a few cases a vibronic transition was found to be 50% as strong as an allowed electric-dipole transition within a given  $J$  manifold.

The electronic transitions observed at 77°K and associated with the  ${}^3P_J$ ,  ${}^1I_6$ , and  ${}^1D_2$  levels are reported in Table I. From this data, it is possible to determine

the crystalline-field splitting of the ground-state level  ${}^3H_6$  and the splitting of the excited levels. To interpret the electronic spectrum of the  ${}^3P_1$  and  ${}^3P_0$  levels, the ground Stark level  $\bar{\mu}=0$ , and the levels  $\bar{\mu}=\pm 1$  and  $\bar{\mu}=\pm 2$  of  ${}^3H_6$  are assumed from the experimental evidence obtained from the spectra of other levels wherein transitions from these three lowest  ${}^3H_6$  Stark levels are allowed.

Nearly all the electronic energy levels previously reported<sup>14-16</sup> for the  ${}^1G_4$  and  ${}^3F_J$  levels are in reasonable agreement with the values measured in this present study. The observed crystalline Stark splitting of all levels agrees to within 4  $\text{cm}^{-1}$  with a first-order degenerate perturbation calculation using the crystal-field parameters,  $A_2^0\langle r^2 \rangle = 135.3 \text{ cm}^{-1}$ ,  $A_4^0\langle r^4 \rangle = -71.35 \text{ cm}^{-1}$ ,  $A_6^0\langle r^6 \rangle = -28.80 \text{ cm}^{-1}$ , and  $A_6^6\langle r^6 \rangle = 428.1 \text{ cm}^{-1}$ .

### INTENSITIES OF THE 300°K ABSORPTION SPECTRUM

The sum of the individual Stark-level absorption-line strengths<sup>9</sup> between  $J$  levels split by a small crystalline Stark field perturbation is equal to the absorption line strength between the unsplit  $J$  levels, provided the temperature of the system  $T$  and the over-all crystalline Stark splitting  $\Delta E \ll kT$ . Under these conditions, the Stark-split components of the ground level are equally occupied. This condition is reasonably valid for the  ${}^3H_6$   $J$  level at 300°K, so that an averaging process over the crystal-field expansion parameters can be made. In terms of the oscillator strength<sup>7,19</sup> one may write

$$f = \frac{mc4\pi}{3\hbar\bar{\lambda}(2J+1)} \frac{(n^2+2)^2}{9n} \sum_{\lambda=2,4,6} \Omega_\lambda [\Gamma^{(\lambda)}]^2, \quad (9)$$

where

$$\Omega_\lambda = 2(2\lambda+1) \sum_t (2t+1)^{-1} |A_{t,p}\bar{\Xi}(t,\lambda)|^2 + C(\lambda), \quad (10)$$

and where  $\bar{\lambda}$  is the average wavelength for a given  $J$  level.

In Eq. (10),  $C(2)$ ,  $C(4)$ , and  $C(6)$  represent coefficients which take into account the vibronic-electronic contribution to the line strength, and may be expressed in terms of the normal coordinates of the lattice or complex, the gradient of the crystal field parameters with respect to the normal coordinates, and the density-of-phonon states. The importance of Eq. (9) lies in the fact that total oscillator strengths between  $J$  levels of the  $4f^n$  configuration are specified by only 3 parameters,  $\Omega_2$ ,  $\Omega_4$ , and  $\Omega_6$ . Although the relative signs of the  $A_{t,p}\bar{\Xi}(t,\lambda)$  parameters are not obtained in this way, values of  $\Omega_\lambda$  will give an order of magnitude to the  $A_{t,p}\bar{\Xi}(t,\lambda)$  parameters themselves, and will also indicate to some extent the amount of vibronic-electronic interaction present in the observed spectrum if the  $A_{t,p}\bar{\Xi}(t,\lambda)$  parameters are reasonably temperature-independent and can be determined from the low-temperature data.

TABLE II. Total electric-dipole oscillator strengths for thulium ethyl sulfate at 300°K. The values for  $f_{\text{meas}}$  were determined from the expression

$$f_{\text{meas}} = \frac{mc}{\rho\pi e^2} \int_0^\infty k(\nu) d\nu$$

where  $\int_0^\infty k(\nu) d\nu$  is the measured quantity. The values for  $f_{\text{calc}}$  were calculated from Eq. 9 using the parameters  $\Omega_2 = 0.593 \times 10^{-20} \text{ cm}^2$ ,  $\Omega_4 = 2.248 \times 10^{-20} \text{ cm}^2$  and  $\Omega_6 = 1.251 \times 10^{-20} \text{ cm}^2$ .

$[S'L']J'$	$\bar{\lambda}$ (microns)	$f_{\text{meas}} \times 10^7$	$f_{\text{calc}} \times 10^7$	$*(f_{\text{meas}} - f_{\text{calc}}) \times 10^7$
${}^1S_0$	0.122 <sup>b</sup>	...	0.009 <sup>c</sup>	...
${}^3P_2$	0.262 <sup>b</sup>	32.14	28.47	3.67
${}^3P_1$	0.275 <sup>d</sup>	5.13	6.63	-1.50
${}^3P_0$	0.285 <sup>d</sup>	9.62	3.94	0.73
${}^1I_6$	0.285 <sup>d</sup>		4.95	
${}^1D_2$	0.359 <sup>d</sup>	23.48	25.95	-2.47
${}^1G_4$	0.470 <sup>d</sup>	5.59	4.95	0.64
${}^3F_2$	0.658 <sup>d</sup>	6.10	5.42	0.68
${}^3F_3$	0.695 <sup>d</sup>	28.05	28.05	0.00
${}^3F_4$	0.790 <sup>d</sup>	16.29	16.38	-0.09
${}^3H_5$	1.282 <sup>b</sup>	...	8.98 <sup>c</sup>	...
${}^3H_4$	1.880 <sup>b</sup>	...	9.82 <sup>c</sup>	...
$H_6$	33 <sup>b</sup>	...	0.84 <sup>c</sup>	...

\* The percent deviation between total  $f_{\text{meas}}$  and  $f_{\text{calc}}$  is 7.7%.

<sup>b</sup> Wavelengths are calculated from the "free ion" wave functions.

<sup>c</sup> Calculated  $f$  number is only approximate since the index factor  $(n^2+2)/9n$  is not known experimentally at this wavelength.

<sup>d</sup> Wavelengths are experimental centers of gravity of crystalline Stark split levels.

The total  $f$ -numbers for transitions between the  ${}^3H_6$  ground  $J$ -level and the  ${}^3F_{4,3,2}$ ,  ${}^1G_4$ ,  ${}^1D_2$ ,  ${}^1I_6$ ,  ${}^3P_{2,1,0}$  levels were measured at 300°K and are listed in Table II. The three  $\Omega_\lambda$  parameters were adjusted to minimize the sum of the squares of the deviation between measured and calculated line strengths.

The values of  $n$  are taken from Fig. 1. The values of  $\Gamma^{(\lambda)}$  are reported in Table III, and are based on the intermediate-coupling free-ion wavefunctions for  $\text{Tm}^{3+}$  that are reported in Table IV. The parameters giving the best over-all agreement are  $\Omega_2 = 0.593 \times 10^{-20} \text{ cm}^2$ ,  $\Omega_4 = 2.248 \times 10^{-20} \text{ cm}^2$ , and  $\Omega_6 = 1.251 \times 10^{-20} \text{ cm}^2$ , and predict the oscillator strengths reported in Table II.

### INTENSITIES OF THE LOW-TEMPERATURE ABSORPTION SPECTRUM

The electric-dipole matrix elements given in Eqs. 7 and 8 contain the well-known selection rules for the

TABLE III. Intermediate coupling values of  $\Gamma^{(\lambda)}(\gamma f^n [SL]J \| U^{(\lambda)} \| \gamma f^n [S'L']J')$  for thulium ethyl sulfate with  $[SL]J = {}^3H_6$ .

$[S'L']J'$	$\lambda=2$	$\lambda=4$	$\lambda=6$
${}^1S_0$			0.00890
${}^3P_2$		-0.51635	0.15252
${}^3P_1$			0.35187
${}^3P_0$			-0.27583
${}^1I_6$	0.10745	0.20567	0.12085
${}^1D_2$		0.55768	-0.30561
${}^1G_4$	-0.21535	-0.27330	0.09981
${}^3F_2$		-0.00079	0.50766
${}^3F_3$		-0.56227	0.91675
${}^3F_4$	0.49881	0.34337	-0.77979
${}^3H_5$	-0.32758	0.48086	0.79865
${}^3H_4$	0.72626	0.84752	-0.47708
${}^3H_6$	1.12002	-0.82933	-0.87950

TABLE IV. The free-ion wave functions for trivalent thulium.<sup>a</sup>

$[^3H_6] = 0.9953 ^3H_6\rangle + 0.0973 ^1I_6\rangle$
$[^3H_4] = -0.2804 ^3H_4\rangle + 0.7817 ^3F_4\rangle + 0.5567 ^1G_4\rangle$
$[^3H_5] = 1.0000 ^3H_5\rangle$
$[^3F_4] = 0.5395 ^3F_4\rangle + 0.7522 ^3H_4\rangle - 0.3785 ^1G_4\rangle$
$[^3F_3] = 1.0000 ^3F_3\rangle$
$[^3F_2] = -0.8738 ^3F_2\rangle + 0.4654 ^1D_2\rangle + 0.1408 ^3P_2\rangle$
$[^1G_4] = 0.7393 ^1G_4\rangle + 0.5963 ^3H_4\rangle - 0.3128 ^3F_4\rangle$
$[^1D_2] = 0.6400 ^1D_2\rangle + 0.6284 ^3P_2\rangle + 0.4422 ^3F_2\rangle$
$[^1I_6] = 0.9953 ^1I_6\rangle - 0.0973 ^3H_6\rangle$
$[^3P_0] = 0.9719 ^3P_0\rangle - 0.2353 ^1S_0\rangle$
$[^3P_1] = 1.0000 ^3P_1\rangle$
$[^3P_2] = -0.7650 ^3P_2\rangle + 0.2023 ^3F_2\rangle + 0.6114 ^1D_2\rangle$
$[^1S_0] = 0.9719 ^1S_0\rangle + 0.2353 ^3P_0\rangle$

<sup>a</sup> The wavefunctions are calculated in intermediate coupling using the following Racah and spin-orbit parameters:

$$\begin{aligned} E^1 &= 6722.2 \text{ cm}^{-1}, \\ E^2 &= 33.88 \text{ cm}^{-1}, \\ E^3 &= 663.45 \text{ cm}^{-1}, \\ \zeta &= 2667.9 \text{ cm}^{-1}. \end{aligned}$$

$\bar{\mu}$ ,  $\bar{\mu}' : \Delta\bar{\mu} = \pm 2, \pm 4(\sigma)$ ,  $\Delta\bar{\mu} = \pm 3(\pi)$  and  $0^\pm \rightarrow 3^\mp$ ,  $\Delta J$  even;  $0^\pm \rightarrow 3^\pm$ ,  $\Delta J$  odd. Thus, in the 4.2°K spectrum of the  $J$  levels studied, only nine electric-dipole transitions are allowed by the  $D_{3h}$  perturbation potential from the  $\bar{\mu}=0$  ground Stark component. By thermally populating the first excited Stark component  $\bar{\mu} = \pm 1$  at 32  $\text{cm}^{-1}$ , an additional seventeen transitions are expected. If the temperature of the crystal is increased to 77°K, the absorption spectrum of a given  $J$  level becomes so dense due to temperature-dependent transitions that many absorption peaks overlap sufficiently to make it difficult to measure integrated absorption coefficients with any accuracy. The spectrum studied at the equilibrium temperature of 23°K appears to be nearly optimum for quantitative intensity measurements since only the two lowest lying Stark components are occupied.

Expressions for the line strengths of transitions originating from a  $J=6$ ,  $\bar{\mu}=0$  or  $\bar{\mu} = \pm 1$  level and terminating on any of the Stark components of the  $^3P_{2,1,0}$ ,  $^1I_6$ ,  $^1D_2$ ,  $^1G_4$ ,  $^3F_{2,3,4}$   $J$  levels were calculated from Eqs. (7) and (8). Certain linear combinations of the four parameters  $A_{33}\Xi(3,4)$ ,  $A_{53}\Xi(5,4)$ ,  $A_{53}\Xi(5,6)$ , and  $A_{73}\Xi(7,6)$  recur in the expansion for the line strengths in  $D_{3h}$  symmetry as expressed by the  $\Lambda_j$ ,  $J=1 \cdots 6$  of Table V, and their introduction simplifies the fitting

TABLE V. Linear combinations of  $A_{t,3}\Xi(t,\lambda)$  parameters.

$\Lambda_1 = A_{33}\Xi(3,4) + 28(55^{-1/2})A_{53}\Xi(5,4)$
$\Lambda_2 = A_{33}\Xi(3,4) + (55^{-1/2})A_{53}\Xi(5,4)$
$\Lambda_3 = A_{53}\Xi(5,6) + (33/7)^{1/2}A_{73}\Xi(7,6)$
$\Lambda_4 = A_{53}\Xi(5,6) + (2/15)(33/7)^{1/2}A_{73}\Xi(7,6)$
$\Lambda_5 = A_{33}\Xi(3,4) - 8(55^{-1/2})A_{53}\Xi(5,4)$
$\Lambda_6 = -A_{53}\Xi(5,6) + \frac{1}{3}(11/21)^{1/2}A_{73}\Xi(7,6)$

procedure. Although it appears at first that four  $A_{t3}\Xi(t,\lambda)$  parameters are replaced with six  $\Lambda_j$  parameters, the quantities  $\Lambda_5$  and  $\Lambda_6$  are linearly dependent on  $\Lambda_1$ ,  $\Lambda_2$  and  $\Lambda_3$ ,  $\Lambda_4$ , respectively.

The integrated absorption coefficients were measured at 23°K for 17 crystalline Stark level transitions terminating on the  $^3P_2$ ,  $^3P_1$ ,  $^1I_6$ ,  $^1D_2$ ,  $^1G_4$ , and  $^3F_2$   $J$  levels. The measured oscillator strengths  $f_{\text{meas}}$ , corresponding to each observed transition, are listed in Table VI. The calculated line-strength expressions corresponding to the measured transitions were evaluated using the appropriate intermediate-coupled  $\Gamma^{(\lambda)}$  of Table III, and the crystal-field wave functions of Table VII. The best set of parameters  $A_{t3}\Xi(t,\lambda)$  was determined by a mini-

TABLE VI. Electric-dipole oscillator strengths for thulium ethyl sulfate at 23°K.

$[S'L']J'$ of terminal level	Crystal quantum trans. $\bar{\mu} \rightarrow \bar{\mu}'$	$f_{\text{meas}} \times 10^7$	$f_{\text{calc}} \times 10^7$	$^a(f_{\text{meas}} - f_{\text{calc}}) \times 10^7$
$^1D_2$	$\pm 1 \rightarrow \pm 1$	10.41	10.50	-0.09
	$0 \rightarrow \pm 2$	0.88	0.75	0.13
	$\pm 1 \rightarrow \pm 2$	2.10	1.55	0.55
$^3P_1$	$\pm 1 \rightarrow \pm 1$	2.85	1.17	1.68
	$0 \rightarrow \pm 2$	1.39	1.39	0.00
$^3P_2$	$\pm 1 \rightarrow \pm 1$	8.40	8.82	-0.42
	$\pm 1 \rightarrow \pm 2$	3.82	3.82	0.00
	$0 \rightarrow \pm 2$	0.33	0.26	0.07
$^3F_2$	$\pm 1 \rightarrow \pm 1$	0.71	0.75	-0.04
	$\pm 1 \rightarrow \pm 2$	1.64	1.90	-0.26
	$0 \rightarrow \pm 2$	0.33	0.26	0.07
$^1G_4$	$\pm 1 \rightarrow \pm 2L$	1.52	2.36	-0.84
	$0 \rightarrow 3L$	0.97	0.29	0.64
	$^b 0 \rightarrow \pm 2L$	0.55	0.46	0.09
	$^b 0 \rightarrow \pm 2H$	4.66	4.75	-0.09
	$0 \rightarrow 3H$	0.38	0.29	0.09
$^1I_6$	$^b 0 \rightarrow \pm 2L$	1.68	1.90	-0.22
	$0 \rightarrow \pm 2H$			
	$0 \rightarrow 3H$	0.38	0.29	0.09

<sup>a</sup> The average percent deviation between total measured and calculated  $f$  numbers is 12.3%.

<sup>b</sup> Transitions used to determine value for  $A_{33}\Xi(3,2)$ .

The values for  $f_{\text{calc}}$  were calculated using the parameters:

$$\begin{aligned} A_{33}\Xi(3,2) &= 23.13 \times 10^{-11} \text{ cm}, \\ A_{33}\Xi(3,4) &= -3.52 \times 10^{-11} \text{ cm}, \\ A_{53}\Xi(5,4) &= 5.35 \times 10^{-11} \text{ cm}, \\ A_{53}\Xi(5,6) &= -2.46 \times 10^{-11} \text{ cm}, \\ A_{73}\Xi(7,6) &= 2.25 \times 10^{-11} \text{ cm}. \end{aligned}$$

mization calculation. The percent deviation between total measured and calculated  $f$  numbers is 12.3% for 17 measured transitions and is commensurate with the experimental errors. Although quantitative intensity measurements were not possible for the  $^3F_3$  and  $^3F_4$  levels, reasonable values were predicted using these parameters.

The selection rules predict that transitions from  $^3H_6$  (lower energy  $\bar{\mu}=3$ ) to  $^3P_0$  ( $\bar{\mu}=0$ ) and  $^3H_6$  ( $\bar{\mu}=0$ , ground state) to  $^1G_4$  (higher energy  $\bar{\mu}=3$ ) are forbidden. To see whether or not the transition to the  $^3P_0$  is truly forbidden or only very weak, the path length was increased using a crystal 20-mm long. No evidence for an additional crystalline Stark transition was observed.

However, in the presence of a strong magnetic field, a weak  $\pi$  line appeared that placed a level in the  ${}^3H_6$  manifold at  $156\text{ cm}^{-1}$ . This level was also observed in the proper polarization in the  ${}^3P_2$  spectrum where transitions to  ${}^3P_2$  ( $\bar{\mu}=0$  and  $\pm 1$ ) are allowed from both  $\bar{\mu}=3$  levels of  ${}^3H_6$ . Similarly, it appears that the transition previously assigned  ${}^3H_6$  ( $\bar{\mu}=0$  ground state) to  ${}^1G_4$ , (higher energy  $\bar{\mu}=3$ ) is vibronic rather than electronic in origin.<sup>14-16</sup>

### DISCUSSION AND COMMENTS

A true minimum in this five-dimensional space is assured if all possible values of the set  $A_{t,\lambda}\Xi(t,\lambda)$  are tried. Unless a good initial estimate of the parameters can be made, false minima could easily occur when fitting all 17 transition amplitudes simultaneously. In principle, it should be possible to reduce the number of phenomenological parameters from five to three since the ratios  $A_{33}\Xi(3,4)/A_{33}\Xi(3,2)$  and  $A_{53}\Xi(5,4)/A_{53}\Xi(5,6)$  are independent of the lattice sum values for  $A_{33}$  and  $A_{53}$ , and may be estimated provided the radial integrals and energy denominators are known.

TABLE VII. Some crystalline-field wave functions not diagonal in  $J_z$ .

$[\text{}^S L_J]; \mu = \sum J_z A(\mu, J_z)  J_z\rangle^a$
$[\text{}^3H_6]; \mu=0L^b = 0.116 -6\rangle + 0.116 +6\rangle + 0.986 0\rangle$
$[\text{}^3H_6]; \mu=\pm 1L = 0.289 -5\rangle + 0.957 1\rangle$ $0.957 5\rangle + 0.289 -1\rangle$
$[\text{}^3F_4]; \mu=\pm 2L = 0.814 -4\rangle + 0.581 +2\rangle$
$[\text{}^3F_4]; \mu=\pm 2L = 0.814 -4\rangle + 0.581 +2\rangle$ $0.581 -2\rangle + 0.814 +4\rangle$
$[\text{}^3F_4]; \mu=\pm 2H = -0.581 -4\rangle + 0.814 +2\rangle$ $0.581 +4\rangle - 0.814 -2\rangle$
$[\text{}^3F_4]; \mu=3L = 0.707 -3\rangle + 0.707 +3\rangle$
$[\text{}^3F_4]; \mu=3H = -0.707 -3\rangle + 0.707 +3\rangle$
$[\text{}^3F_3]; \mu=3L = 0.707 -3\rangle - 0.707 +3\rangle$
$[\text{}^3F_3]; \mu=3H = 0.707 -3\rangle + 0.707 +3\rangle$
$[\text{}^1G_4]; \mu=\pm 2L = 0.628 -2\rangle - 0.779 +4\rangle$ $0.779 -4\rangle - 0.628 +2\rangle$
$[\text{}^1G_4]; \mu=\pm 2H = 0.779 -2\rangle + 0.628 +4\rangle$ $0.628 -4\rangle + 0.779 +2\rangle$
$[\text{}^1G_4]; \mu=3L = 0.707 -3\rangle - 0.707 +3\rangle$
$[\text{}^1G_4]; \mu=3H = 0.707 -3\rangle + 0.707 +3\rangle$
$[\text{}^1I_6]; \mu=\pm 2H = 0.660 +4\rangle + 0.752 -2\rangle$ $0.660 -4\rangle + 0.752 +2\rangle$
$[\text{}^1I_6]; \mu=\pm 2L = -0.738 +4\rangle + 0.668 -2\rangle$ $0.738 -4\rangle - 0.668 +2\rangle$
$[\text{}^1I_6]; \mu=3H = 0.707 +3\rangle - 0.707 -3\rangle$
$[\text{}^1I_6]; \mu=3L = 0.707 +3\rangle + 0.707 -3\rangle$

<sup>a</sup> These wave functions were determined from 1st-order degenerate perturbation calculations using the crystal-field parameters  $A_4^0(r^2) = 135.3\text{ cm}^{-1}$ ,  $A_4^2(r^4) = -71.35\text{ cm}^{-1}$ ,  $A_6^0(r^6) = -28.80\text{ cm}^{-1}$ , and  $A_6^4(r^6) = 428.1\text{ cm}^{-1}$ .

<sup>b</sup> The letters  $L$  and  $H$  refer to the lower or higher in energy of two Stark components within a given  $J$  level that have the same crystal quantum number. In  $D_{2h}$  symmetry the crystal-quantum state is labeled  $\bar{\mu}$ .

TABLE VIII. Radial integrals and energy denominators for  $\text{Tm}^{3+}$  and  $\text{Eu}^{3+}$ . The radial integrals for  $\text{Tm}^{3+}$  were calculated by Rajnak.<sup>29</sup> The values for the radial integrals for  $\text{Eu}^{3+}$  are interpolated from the calculated radial integrals for  $\text{Pr}^{3+}$  and  $\text{Tm}^{3+}$ . The  $\Delta E_{5d}$  energy differences are linearly interpolated values from the experimental data for  $\text{Ce}^{3+}$  and  $\text{Yb}^{3+}$  due to Dieke *et al.*<sup>24</sup> The  $\Delta E_{5g}$  energy differences are linearly interpolated values from Ridley's<sup>30</sup> calculated values for  $\text{Pr}^{3+}$  and  $\text{Tm}^{3+}$ . Radial integrals are in atomic units, and energies in  $\text{cm}^{-1}$ .

Integral	$\text{Tm}^{3+}$	$\text{Eu}^{3+}$
$\langle 4f r 5d\rangle$	0.583	0.673
$\langle 4f r^2 5d\rangle$	2.45	4.26
$\langle 4f r^6 5d\rangle$	16.5	36.9
$\langle 4f r^4 4f\rangle$	1.57	3.83
$\langle 4f r^6 4f\rangle$	7.31	26.7
$\langle 4f r^8 4f\rangle$	62	325
Energy, $\Delta E_{n'l}$		
$\Delta E_{5d}$	95 000	71 000
$\Delta E_{5g}$	200 000	150 000

Unfortunately, only estimates of the energy denominators<sup>24</sup> are available and only values for the matrix elements of  $r^n$  between  $4f$  and  $5d$  orbitals have been reported<sup>29</sup> to date and are summarized in Table VIII. Since the  $n'd$  orbitals from  $n' > 6$  lie considerably higher than the  $5d$  orbital, their spatial overlap with the  $4f$  orbital is presumably much smaller, so that  $d$  orbitals for  $n' > 5$  are neglected in estimating the  $\Xi(t,\lambda)$  parameters. No radial integrals for  $g$  orbitals have been calculated, so that some approximation must be made. Since the estimated energy of the  $5g$  orbital is  $200\,000\text{ cm}^{-1}$  above the ground state, we assume that the remaining  $n'g$  orbitals occupy an energy width small compared to this energy, and impose the closure relation<sup>7</sup>  $\sum_{n'} \langle 4f|r|n'g\rangle \langle n'g|r^t|4f\rangle \sim \langle 4f|r^{t+1}|4f\rangle$ . Based on these approximations, the results for  $\text{Tm}^{3+}$  are  $A_{33}\Xi(3,4)/A_{33}\Xi(3,2) = 1.022$ , and  $A_{53}\Xi(5,4)/A_{53}\Xi(5,6) = 0.59$ . By using these ratios, the transition amplitudes then depend only on three parameters,  $A_{33}\Xi(3,2)$ ,  $A_{53}\Xi(5,4)$ , and  $A_{73}\Xi(7,6)$ . In order to test these ratios in the simplest way, only the transitions allowed from  $\bar{\mu}=0$  (whose relative oscillator strengths are independent of the crystal temperature) were calculated under these restraints. The three parameters were varied freely, and the sum of the squares of the deviations between measured and calculated amplitudes was minimized. With the best set of three parameters, the average deviation between calculated and measured  $f$  numbers was 30%. However, when the  $f$  numbers with  $\bar{\mu}=\pm 1$  were calculated with these parameters, the values obtained were mostly too large, in some cases by factors of 50, well outside experimental errors associated with the measured oscillator strengths. To see whether or not these constraints would be more successful in the only other ethyl sulfate system studied so far, the ratio  $A_{33}\Xi(3,4)/A_{33}\Xi(3,2)$  was determined for  $\text{Eu}(\text{C}_2\text{H}_5\text{SO}_4)_3 \cdot 9\text{H}_2\text{O}$  by interpolating values for the  $\text{Eu}^{3+}$  radial

<sup>29</sup> K. Rajnak, J. Chem. Phys. 37, 2440 (1962).



integrals from Rajnak's  $\text{Pr}^{3+}$  and  $\text{Tm}^{3+}$  results.<sup>29</sup> Using the values appearing in Table VIII,<sup>30</sup> the calculated ratio is 0.9 and if imposed predicts intensities considerably different than those observed, which Axe<sup>9</sup> accounted for by setting  $A_{33\Xi}(3,4)=0$  and varying only  $A_{33\Xi}(3,2)$  and  $A_{53\Xi}(5,4)$ .

Until more complete information is available regarding excited configurations, it was decided to vary all five parameters freely to see if any better agreement was possible. It happens that five of the measured transitions are specified by only two quantities,  $\Lambda_5$  and  $\Lambda_6$ , and these transitions were considered first. A simple evaluation gives the only values and signs of  $\Lambda_5$  and  $\Lambda_6$  which account for all the observed amplitudes. Using these results,  $\Lambda_2$  and  $\Lambda_4$  are then written in terms of  $\Lambda_1$  and  $\Lambda_3$ , and the remaining twelve transition-amplitude expressions then appear in terms of  $A_{33\Xi}(3,2)$ ,  $\Lambda_1$ , and  $\Lambda_3$ .

Of these 12 transitions, nine are also independent of  $A_{33\Xi}(3,2)$ . Again it is possible to vary the two quantities  $\Lambda_1$  and  $\Lambda_3$  for all possible signs and values for these nine transitions and find only one set of values which at all comes close to predicting the observed values. With parameters  $\Lambda_1$ ,  $\Lambda_2$ ,  $\Lambda_3$ , and  $\Lambda_4$  thus estimated, it is possible to use these as starting parameters in a fitting of the 14 transitions not dependent on  $A_{33\Xi}(3,2)$ . The sum of the squares of the differences between the measured and calculated *amplitudes* was minimized by varying the  $\Lambda_j$ ,  $j=1\cdots 4$ . Finally, the parameter  $A_{33\Xi}(3,2)$  was varied, leaving  $\Lambda_{1-4}$  fixed and the remaining three amplitudes were fit. The final  $\Lambda_j$  differed only slightly from the estimated starting set. The final set of parameters used to calculate the  $f$  numbers appearing in Table VI are

$$\begin{aligned} A_{33\Xi}(3,2) &= 23.13 \times 10^{-11} \text{ cm}, \\ A_{3,3\Xi}(3,4) &= -3.52 \times 10^{-11} \text{ cm}, \\ A_{5,3\Xi}(5,4) &= 5.35 \times 10^{-11} \text{ cm}, \\ A_{5,3\Xi}(5,6) &= -2.46 \times 10^{-11} \text{ cm}, \end{aligned}$$

and

$$A_{7,3\Xi}(7,6) = 2.25 \times 10^{-11} \text{ cm}.$$

If the expressions  $A_{t,p\Xi}(t,\lambda)$  do not vary greatly with temperature, we can learn something about the vibronic contribution to the total absorption spectrum by using the  $A_{t,p\Xi}(t,\lambda)$  parameters determined from the low-temperature data to calculate the static contribution to the oscillator strengths in the 300°K temperature spectrum. Calling the terms as derived from the  $A_{t,p\Xi}(t,\lambda)$  parameters themselves  $\Omega_\lambda'$ , we find that  $\Omega_2' = 7.64 \times 10^{-20} \text{ cm}^2$ ,  $\Omega_4' = 0.79 \times 10^{-20} \text{ cm}^2$ , and  $\Omega_6' = 0.245 \times 10^{-20} \text{ cm}^2$ . On comparing these values with  $\Omega_\lambda$ , we find  $\Omega_4' < \Omega_4$  and  $\Omega_6' < \Omega_6$  as might be expected, indicating that the vibronic contribution terms at 300°K,  $C(4)$  and  $C(6)$ , are approximately 2 and 4 times larger than the static contributions. On the other

hand  $\Omega_2'$  is greater than  $\Omega_2$  by a factor of 13. The expression  $\Omega_2'$  involves only the  $A_{33\Xi}(3,2)$  term.

The magnitude of the  $\Omega_\lambda$  for thulium ethyl sulfate can be compared with the corresponding  $\Omega_\lambda$  found by Axe<sup>9</sup> for EuES:  $\Omega_2 = 0.14 \times 10^{-20} \text{ cm}^2$  and  $\Omega_4 = 2.10 \times 10^{-20} \text{ cm}^2$ , and the  $\Omega_\lambda$  found by Judd<sup>7</sup> for  $\text{ErCl}_3$  solution:  $\Omega_2 = 1.41 \times 10^{-20} \text{ cm}^2$ ,  $\Omega_4 = 2.47 \times 10^{-20} \text{ cm}^2$ , and  $\Omega_6 = 2.12 \times 10^{-20} \text{ cm}^2$ . The  $\Omega_4$  and  $\Omega_6$  parameters are all quite similar, whereas the  $\Omega_2$  parameters vary as much as an order of magnitude. The static part of  $\Omega_2$  depends only on  $A_{33\Xi}(3,2)$  and not the other  $A_{t,p\Xi}(t,\lambda)$ . Since the four parameters  $A_{33\Xi}(3,4)$ ,  $A_{53\Xi}(5,4)$ ,  $A_{53\Xi}(5,6)$ , and  $A_{73\Xi}(7,6)$  were determined independently of  $A_{33\Xi}(3,2)$ , their values are independent of any anomalous effects associated with  $A_{33\Xi}(3,2)$ . Judd<sup>7</sup> noted that certain transitions for which  $\Delta J \leq 2$  and which depend on  $A_{33\Xi}(3,2)$  are hypersensitive to changes in the ion environment. Recently<sup>31</sup> it has been suggested that this hypersensitivity is most likely not associated with the electric-dipole operator, but rather with the electric quadrupole operator, which may be nonzero between states of the same parity. While the calculated intensities of electric-quadrupole transitions are several orders of magnitude weaker than the calculated electric-dipole intensities, Jørgensen and Judd<sup>31</sup> suggest that the electromagnetic field induces an asymmetrical distribution of dipoles in the medium surrounding the impurity ion, producing a large electric-field gradient across the ion. As a result, the intensities of quadrupole transitions may be enormously enhanced. The expression for the electric dipole oscillator strength has the same angular dependence for the  $\lambda=2$  term as the expression for the electric quadrupole oscillator strength,<sup>3</sup> and might easily lead to a value for  $A_{33\Xi}(3,2)$  larger than would be expected otherwise. Our value of  $A_{33\Xi}(3,2)$  was determined by fitting three  $\bar{\mu}=0 \rightarrow \pm 2$  transitions which appear in  $\sigma$ -polarization. The electric quadrupole selection rules for  $D_{3h}$  symmetry allow  $\sigma$ -polarized electric quadrupole transitions between  $\bar{\mu}=0$  and  $\bar{\mu}=\pm 2$  Stark levels, consistent with the possibility that enhanced electric quadrupole transitions may be in part contributing to the observed electronic spectra.

The experimentally determined ratios  $A_{33\Xi}(3,4)/A_{33\Xi}(3,2) = -0.15$  and  $A_{53\Xi}(5,4)/A_{53\Xi}(5,6) = -2.08$  do not agree with the ratios calculated using free-ion excited radial wave functions. Therefore interpretation of the parameters will require more detailed knowledge of the excited ionic states in a crystalline environment and a careful treatment of the lattice sum calculation for the odd-degree terms in ethyl sulfates. However, the fact that the intensities of the observed spectrum ranging over a factor of 40 between 38 000 and 15 000  $\text{cm}^{-1}$  can be accounted for with five phenomenological parameters is an encouraging step toward understanding optical intensities of rare-earth ions in crystals.

<sup>30</sup> E. C. Ridley, Proc. Cambridge Phil. Soc. **56**, 41 (1960).

<sup>31</sup> C. K. Jørgensen and B. R. Judd, Mol. Phys. **8**, 281 (1964).